

Association of dopamine depletion and cholinergic basal forebrain atrophy with brain metabolism and cognition in Parkinson's disease

Journal of Parkinson's Disease

1–12

© The Author(s) 2025

Article reuse guidelines:

sagepub.com/journals-permissions

DOI: 10.1177/1877718X251396322

journals.sagepub.com/home/pkn



Jung Hyun Lee¹ , Mina Park², Sung Jun Ahn², Jae Hoon Lee³ , Young Hoon Ryu³, Han Soo Yoo¹ and Chul Hyoung Lyoo¹

Abstract

Background: Cognitive dysfunction is one of the most debilitating non-motor symptoms of Parkinson's disease (PD). This study aimed to explore the interplay between altered neurotransmitter activities, including dopamine and acetylcholine, and brain metabolism in cognitive decline in PD.

Methods: We enrolled 172 PD patients (mean \pm SD age 69.8 ± 8.6 years; 93 females) who underwent brain magnetic resonance imaging, *N*-(3-[¹⁸F]fluoropropyl)-2 β -carbomethoxy-3 β -(4-iodophenyl) nortropine (¹⁸F-FP-CIT) positron emission tomography (PET), ¹⁸F-fluorodeoxyglucose (FDG) PET, and neuropsychological testing. General linear models and mediation analyses were used to investigate the association between striatal dopamine transporter (DAT) availability or basal forebrain (BF) volume, brain metabolism, and domain-specific cognitive scores.

Results: A significant relationship between caudate dopamine depletion and posterior BF atrophy was found in PD patients. Caudate and putaminal dopamine depletion were associated with altered brain metabolism in regions where PD patients showed decreased metabolism compared with healthy controls, whereas atrophy in the posterior BF was associated with hypometabolism in the lateral prefrontal, orbitofrontal, inferior parietal, and lateral temporal cortices as well as in the precuneus, with a significant interaction between caudate DAT availability and posterior BF volume. Caudate dopamine depletion was associated with visuospatial, memory, and executive dysfunction, whereas posterior BF atrophy was additionally associated with attention. Mediation analyses revealed that visuospatial dysfunction was associated with caudate dopamine depletion or posterior BF atrophy via altered brain metabolism, while executive dysfunction was linked to both directly and through metabolism changes.

Conclusions: Caudate dopaminergic and posterior BF cholinergic deficits are interrelated and affect cognition in a domain-specific manner, either directly or through the mediation of altered brain metabolism.

Keywords

cognition, metabolism, basal forebrain, dopamine, parkinson's disease

Received: 18 May 2024; accepted: 20 November 2024

Introduction

Parkinson's disease (PD) presents with characteristic motor symptoms of bradykinesia, rigidity, rest tremor, and gait disturbance caused by nigrostriatal dopamine neuronal degeneration.¹ However, it is also accompanied by various non-motor symptoms, such as sleep disturbance, psychiatric symptoms, and autonomic dysfunction, which are attributable to the disruption of other neurotransmitter circuits including the serotonergic, cholinergic, and noradrenergic systems.² One of the most debilitating non-motor symptoms is cognitive decline. Studies have reported that

¹Department of Neurology, Gangnam Severance Hospital, Yonsei University College of Medicine, Seoul, South Korea

²Department of Radiology, Gangnam Severance Hospital, Yonsei University, College of Medicine, Seoul, South Korea

³Department of Nuclear Medicine, Gangnam Severance Hospital, Yonsei University, College of Medicine, Seoul, South Korea

Corresponding author:

Han Soo Yoo, Department of Neurology, Gangnam Severance Hospital, Yonsei University College of Medicine, 20 Eonjuro 63-gil, Gangnam-gu, Seoul, South Korea.

Email: omsavior7@gmail.com

[†]These authors contributed equally to this work.



Creative Commons Non Commercial CC BY-NC: This article is distributed under the terms of the Creative Commons Attribution-NonCommercial 4.0 License (<https://creativecommons.org/licenses/by-nc/4.0/>) which permits non-commercial use, reproduction and distribution of the work without further permission provided the original work is attributed as specified on the SAGE and Open Access page (<https://us.sagepub.com/en-us/nam/open-access-at-sage>).

approximately 40% of PD patients present with mild cognitive impairment at baseline,³ and up to 80% eventually develop dementia.⁴ Such cognitive deterioration is closely associated with mortality.^{5,6}

Various mechanisms underlying cognitive dysfunction in PD have been suggested, including misfolded proteins in limbic and cortical structures, neuroinflammation, and genetic contributions.⁷ Another significant determinant is the alteration of neurotransmitter systems, especially the dopaminergic and cholinergic pathways. Studies have consistently reported an association between striatal dopamine depletion, especially in the caudate, and executive dysfunction in PD patients,^{4,8} which is believed to reflect frontostriatal dopaminergic deterioration in early PD. Meanwhile, mounting evidence indicates that compromised cholinergic neurons in the basal forebrain (BF) are responsible for cognitive impairment in PD as well.^{9,10} It has been postulated that the disintegration and dysfunction of BF cholinergic neurons that are particularly vulnerable to PD pathology¹¹ alter cholinergic projections to the brain cortex and subsequently manifest as cognitive decline in PD.^{12,13} Although the individual roles of dopaminergic and cholinergic denervation in cognition have been investigated, the interaction and integrative effects of these two major neurotransmitter systems and their clinical implications are yet to be determined.

Discrete changes in brain metabolism assessed by ¹⁸F-fluorodeoxyglucose (FDG) positron emission tomography (PET) are recognized as a biomarker for neurodegeneration¹⁴ and are closely associated with cognition in PD.¹⁵ Our group has previously demonstrated that such changes in brain metabolism were linked to striatal dopamine depletion, potentially mediating the relationship between dopaminergic dysfunction and cognitive decline.¹⁶ However, PD patients with atrophy in the nucleus basalis of Meynert also exhibited reduced metabolism in the parietal and occipital cortices both at baseline and longitudinally.¹⁷ Thus we found it necessary to consider dysfunctions of dopaminergic and cholinergic systems together to understand PD-specific metabolic changes and their role in PD.

Given that striatal dopamine depletion and BF cholinergic denervation are associated with brain metabolism and cognition, respectively, in PD, we hypothesized that striatal dopaminergic and BF cholinergic dysfunctions are closely connected, driving changes in brain metabolism and subsequently leading to cognitive decline. Therefore, we explored the relationship between striatal dopamine transporter (DAT) availability, cholinergic BF volume, brain metabolism, and cognitive impairment in patients with PD.

Methods

Study participants

172 patients from the “PD FDG cohort” at the Movement Disorders Clinic of Gangnam Severance Hospital were

included. The “PD FDG cohort” had been enrolling patients with PD who had undergone brain magnetic resonance imaging (MRI), *N*-(3-[¹⁸F]fluoropropyl)-2 β -carbomethoxy-3 β -(4-iodophenyl) nortropine (¹⁸F-FP-CIT) positron emission tomography (PET), ¹⁸F-FDG PET, and a detailed neuropsychological testing (described below) from May 2022. All patients met the MDS clinical diagnostic criteria for clinically probable PD.¹⁸ As an absolute exclusion criterion, patients who did not exhibit reduced DAT availability in the putamen were excluded. Drug-naïve PD patients were followed up for at least 6 months to confirm that they showed a clear response to dopaminergic treatment. All assessments were conducted within 6 months. Patients with other causes of cognitive impairment or motor deficits, such as epilepsy, psychiatric disorders, normal pressure hydrocephalus, and structural brain lesions (e.g., tumor, hemorrhage, severe white matter hyperintensity,¹⁹ or multiple lacunes) observed on brain MRI were excluded from this study.

We also enrolled 40 age- and sex-matched healthy controls (HC) to compare regional brain metabolism with that of the PD group. Healthy participants had no history of neurological illness or abnormal signs on neurological examination and had scores of 26 or more on the Korean version of the Mini-Mental State Examination. Healthy controls also underwent ¹⁸F-FP-CIT PET, ¹⁸F-FDG PET, and brain MRI within 6 months.

Neuropsychological evaluation

All participants underwent a standardized neuropsychological battery called the Seoul Neuropsychological Screening Battery,²⁰ which assesses attention, language, visuospatial, memory, and executive domain functions. Standardized z-scores were computed for all relevant tests using age- and education-matched norms. The following tests were included in our analyses: digit span forward and backward; the Korean version of the Boston Naming Test (K-BNT); the copying item of the Rey-Osterrieth Complex Figure Test (RCFT); immediate recall, 20-min delayed recall, and recognition items of the RCFT and Seoul Verbal Learning Test (SVLT); and the semantic and phonemic Controlled Oral Word Association Test (COWAT) and Stroop color reading test.

Acquisition and image processing of brain MRI and PET

For the structural imaging in the PD patients, T1-weighted sagittal MR images were acquired with a 3D magnetization prepared-rapid gradient-echo sequence (TR/TE = 2300/2.98 ms, flip angle = 9°, 248 × 256 × 176 matrix, 1 mm iso-voxel) in a 3.0 Tesla MR scanner (MAGNETOM Vida, Siemens Healthineers, Erlangen, Germany). For healthy controls, T1-weighted axial MR images were acquired

with 3D-spoiled gradient-recalled sequences (TR/TE = 6.8/1.6–11.0 ms, flip angle = 20°, 512 × 512 × 176 matrix, voxel size = 0.4688 × 0.4688 × 1 mm) in a 3.0 T GE Signa EXCITE scanner (GE Medical Systems, Milwaukee, WI, USA).

All ^{18}F -FDG and ^{18}F -FP-CIT PET images were acquired in a Biograph 40 TruePoint PET/CT scanner (Siemens Medical Solutions; Malvern, PA, USA). We first applied a head holder to minimize head motion and then acquired brain computed tomography (CT) for later attenuation correction. Subsequently, PET images were acquired for 10 min at 50 min after the injection of ^{18}F -FDG and at 3 h after the injection of ^{18}F -FP-CIT. Finally, PET images were reconstructed with ordered-subsets expectation maximization algorithm (512 × 512 × 110 matrix, voxel size = 0.668 × 0.668 × 2 mm).

Image processing steps for MR. We used the statistical parameter mapping 12 (SPM12, Wellcome Centre for Human Neuroimaging, London, UK) and in-house software implemented in MATLAB 2021a (MathWorks, Natick, MA, USA) for the preprocessing of images and the FreeSurfer 7.2 (Massachusetts General Hospital, Harvard Medical School; <http://surfer.nmr.mgh.harvard.edu>) for the cortical and subcortical segmentation and mapping of data on cortical surface.

Inhomogeneity-corrected T1-weighted MR images were first resliced to our in-house standard 1 mm isovoxel space in 181 × 217 × 181 matrix and then segmented into gray matter (GM) and white matter (WM). Subsequently, the segments were spatially normalized to our in-house diffeomorphic anatomical registration through exponentiated lie algebra (DARTEL) template in 181 × 217 × 181 matrix with 1 mm isovoxels. We used a standard BF volume-of-interest (VOI) based on post-mortem *in cranio* MRI and histology.²¹ By overlaying the standard BF VOI on the spatially normalized and modulated individual T1 images, we measured subregional BF volumes and merged them into two distinct subdivisions with related functions.²² As a result, we obtained anterior [Ch1/2 (medial septal nucleus and vertical limb of the diagonal band of Broca) and Ch3 (horizontal limb of the diagonal band of Broca)] and posterior [cholinergic component of the nucleus basalis Meynert: Ch4ai (anterior intermediate), Ch4al (anterior lateral) and Ch4p (posterior)] BF volumes.

Image processing steps for PET. For the processing of PET images, all PET images were coregistered to the resliced T1 images. By using the FreeSurfer-generated cortical and subcortical segments transferred to our in-house standard space, regional PET uptake values were measured.

For ^{18}F -FP-CIT PET, striatal specific binding ratio (SBR; target region / reference region - 1) values were calculated by using the cerebellar GM as a reference. The target regions included the caudate and putamen. For ^{18}F -FDG PET, we

first obtained a reference region value to create standardized uptake value ratio (SUVR) images. WM reference values were obtained by overlaying the pure WM reference VOI, which is a WM voxel theoretically least affected by spill-over of ^{18}F -FDG uptake from the surrounding GM. To create the pure WM reference VOI, binarized GM segments were smoothed with Gaussian kernel with 5 mm full width at half maximum (FWHM), and then we selected the WM voxels with less than 0.1% probability of contamination by the spill-over from GM. The WM reference VOI were therefore almost invariably in the centrum semiovale. The SUVR images were created using the pure WM reference uptake value. We obtained the values of ^{18}F -FP-CIT SBR-related and BF volume-related brain ^{18}F -FDG SUVR to assess brain metabolic changes related to dopaminergic and cholinergic deficits. To acquire these values, brains were segmented into 34 cortical regions using Desikan-Killiany atlas.²³ Areas of which ^{18}F -FDG SUVR correlated with ^{18}F -FP-CIT SBR or posterior BF volume were selected (Supplemental Table S1), and their weight-average SUVR values were designated as CAUD_{SBR}-related FDG SUVR and pBF_{VOL}-related FDG SUVR.

The SUVR images were spatially normalized by using the flow-field normalizing resliced T1 images and finally smoothed with Gaussian kernel with 10 mm FWHM for the voxel-based statistical analysis. For the visualization of results, statistical significance values of the voxels corresponding to the mid-point of the cortical GM were mapped on the semi-inflated white matter surface.

Statistical analysis

Baseline demographic characteristics were compared using an independent *t*-test and chi-square test. General linear models were used in the following analyses: (1) comparison of the regional brain ^{18}F -FDG SUVR between the PD and HC groups; (2) the association between striatal ^{18}F -FP-CIT SBR (^{18}F -FP-CIT SBR in the caudate [CAUD_{SBR}] and ^{18}F -FP-CIT SBR in the putamen [PUT_{SBR}]) and BF volume (anterior BF volume [aBF_{VOL}] and posterior BF volume [pBF_{VOL}]) in the PD group; (3) the association between striatal ^{18}F -FP-CIT SBR or BF volume and brain ^{18}F -FDG SUVR in the PD group; (4) the association between striatal ^{18}F -FP-CIT SBR or BF volume and cognitive item z-score in the PD group; and (5) the association between striatal ^{18}F -FP-CIT SBR-related or BF volume-related brain ^{18}F -FDG SUVR and cognitive item z-score. In particular, (6) the interaction effects of the pBF_{VOL} and striatal ^{18}F -FP-CIT SBR on the brain ^{18}F -FDG SUVR and cognitive testing scores were assessed. In the group comparison, age at MRI and sex were used as covariates, while in the association analyses, age at MRI, sex, and disease duration were used as covariates. The false discovery rate (FDR) method was applied to correct

voxel-wise multiple analyses for brain mapping and 13 cognitive items. Examples for each analysis are as follows:

1. $FDG\ SUVR = \beta_0 + (\beta_1 \times \text{group}) + (\beta_2 \times \text{age at MR}) + (\beta_3 \times \text{sex})$
2. $aBF_{VOL}\ \text{or}\ pBF_{VOL} = \beta_0 + (\beta_1 \times PUT_{SBR}\ \text{or}\ CAUD_{SBR}) + (\beta_2 \times \text{age at MR}) + (\beta_3 \times \text{sex}) + (\beta_4 \times \text{disease duration})$
3. $FDG\ SUVR = \beta_0 + (\beta_1 \times PUT_{SBR}\ \text{or}\ CAUD_{SBR}\ \text{or}\ aBF_{VOL}\ \text{or}\ pBF_{VOL}) + (\beta_2 \times \text{age at MR}) + (\beta_3 \times \text{sex}) + (\beta_4 \times \text{disease duration})$
4. $\text{Cognitive item z-score} = \beta_0 + (\beta_1 \times PUT_{SBR}\ \text{or}\ CAUD_{SBR}\ \text{or}\ aBF_{VOL}\ \text{or}\ pBF_{VOL}) + (\beta_2 \times \text{age at MR}) + (\beta_3 \times \text{sex}) + (\beta_4 \times \text{disease duration})$
5. $\text{Cognitive item z-score} = \beta_0 + (\beta_1 \times CAUD_{SBR}\text{-related } FDG\ SUVR\ \text{or}\ pBF_{VOL}\text{-related } FDG\ SUVR) + (\beta_2 \times \text{age at MR}) + (\beta_3 \times \text{sex}) + (\beta_4 \times \text{disease duration})$
6. $FDG\ SUVR = \beta_0 + (\beta_1 \times CAUD_{SBR}) + (\beta_2 \times pBF_{VOL}) + (\beta_3 \times \text{age at MR}) + (\beta_4 \times \text{sex}) + (\beta_5 \times \text{disease duration})$

Path analyses were performed to explore the relationship between striatal dopamine depletion or BF atrophy, altered brain metabolism, and cognitive dysfunction. Because the $CAUD_{SBR}$ and pBF_{VOL} showed correlation with both the ^{18}F -FDG SUVR and cognitive function, the $CAUD_{SBR}$ or pBF_{VOL} was used as a predictor. The $CAUD_{SBR}$ -related ^{18}F -FDG SUVR or pBF_{VOL} -related ^{18}F -FDG SUVR was set as a mediator. Since $CAUD_{SBR}$, pBF_{VOL} , and their related ^{18}F -FDG SUVR were commonly correlated with RCFT copy and Stroop color reading z-scores, RCFT copy or Stroop color reading z-score was set as an outcome variable. In addition to the common covariates, the pBF_{VOL} was further adjusted when the $CAUD_{SBR}$ was used as a predictor, while the $CAUD_{SBR}$ was further adjusted when the pBF_{VOL} was used as a predictor to investigate their independent effects on cognition. We used the maximum likelihood method to estimate standardized total, direct, and indirect effects and used a bootstrapping method with 500 resamples to derive 95% confidence intervals and standard errors. The threshold for the modification indices was 4. Indices including the chi-square statistic (χ^2), p-value, comparative fit index (CFI) and the root mean square error of approximation (RMSEA) were used to assess the goodness of fit. A non-significant χ^2 value, CFI value greater than 0.90, and an RMSEA value less than 0.05 were considered indicative of a good fit.

All statistical analyses were performed using SPSS 25 and AMOS 25 (IBM Corp., Armonk, NY) and R software, v.4.2.3 (R Foundation for Statistical Computing, R-project.org). *P*-value or FDR-corrected *P*-value < 0.05 were considered significant.

Table 1. Demographic and clinical characteristics of study participants.

	Healthy controls	PD patients	P-value
Number	40	172	
Basic demographics			
Age at MRI scan, yr	66.76 ± 6.62	69.75 ± 8.63	0.052
Sex, female, n (%)	19 (47.5)	93 (54.1)	0.486
Education, yr		13.04 ± 4.31	
PD-related demographics			
Age at onset, yr		66.12 ± 9.98	
Disease duration, yr		3.63 ± 4.07	
MDS-UPDRS part III total score		25.59 ± 11.53	
Imaging-related parameters			
Caudate SBR	5.82 ± 1.53	3.84 ± 1.29	<0.001
Putaminal SBR	8.12 ± 1.46	3.10 ± 1.03	<0.001
Anterior BF volume	0.24 ± 0.02	0.23 ± 0.03	0.008
Posterior BF volume	0.43 ± 0.04	0.40 ± 0.05	<0.001

Values are expressed as mean ± standard deviation or number (percentage). Abbreviations = BF, basal forebrain; MDS-UPDRS, the Movement Disorder Society-sponsored revision of the Unified Parkinson's Disease Rating Scale; PD, Parkinson's disease; SBR, specific binding ratio

Standard protocol approval, registration, and patient consent

This study was approved by the Institutional Review Board of Gangnam Severance Hospital (No. 3-2024-0106 and 3-2020-0186). Written informed consent was obtained from all patients and HCs. All procedures were performed in accordance with the ethical standards of the 1964 Declaration of Helsinki and its later amendments.

Results

Demographic, clinical, and imaging characteristics

We enrolled 172 patients with PD (mean ± SD age 69.8 ± 8.6 years; 93 females) and 40 healthy controls (mean ± SD age 66.8 ± 6.6 years; 19 females; Table 1) in this study. In patients with PD, the mean age at the onset of motor symptoms was 66.1 years, and the mean disease duration was 3.6 years. The mean total MDS-UPDRS Part III score was 25.6. The PD group had significantly lower $CAUD_{SBR}$, PUT_{SBR} , aBF_{VOL} , and pBF_{VOL} than those in the control group.

Association between the striatal ^{18}F -FP-CIT SBR and BF volume

The $CAUD_{SBR}$ was associated with the aBF_{VOL} ($\beta = 0.187$, $P = 0.015$) and pBF_{VOL} ($\beta = 0.261$, $P = 0.001$;

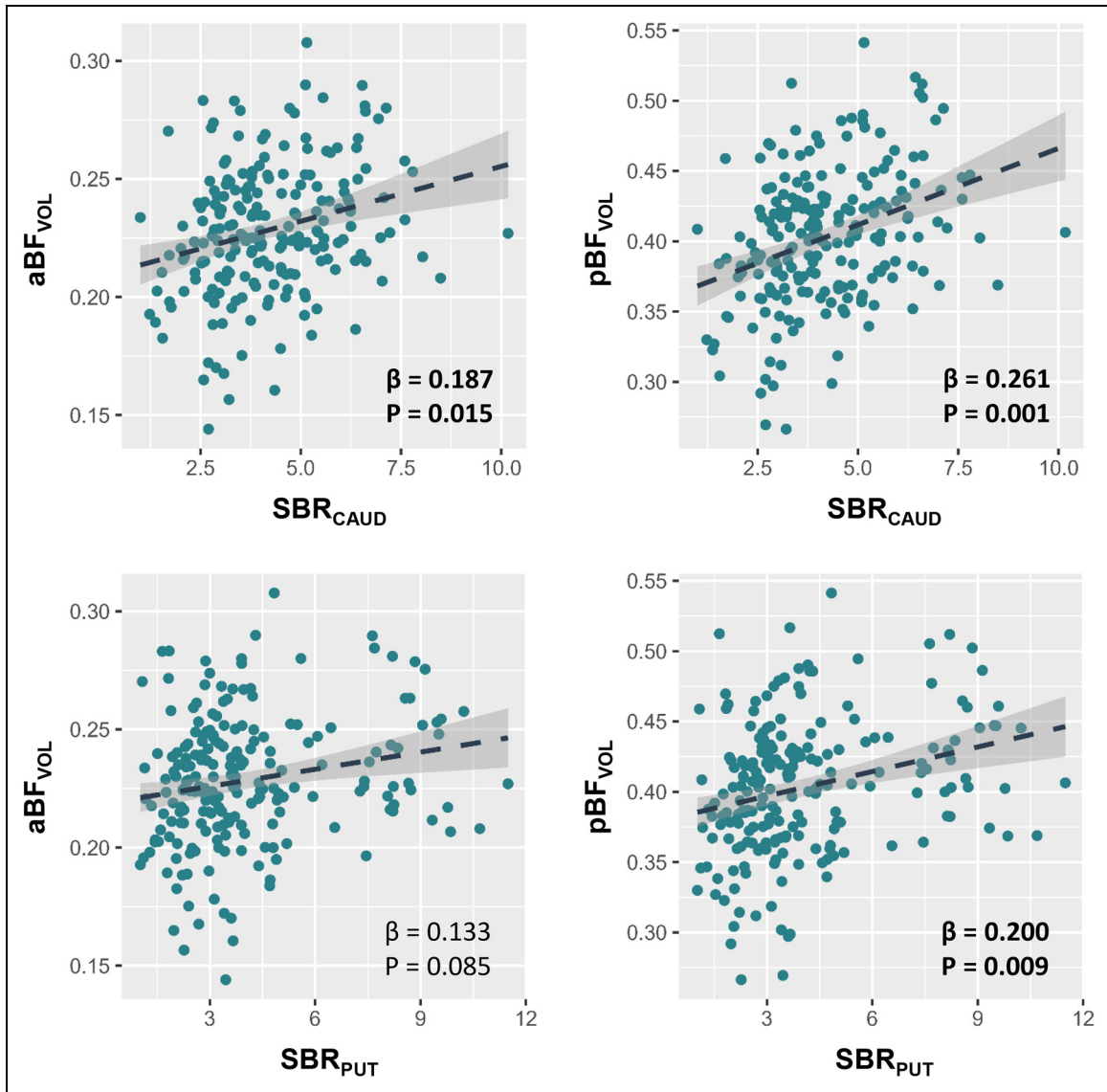


Figure 1. Correlation between the striatal 18F-FP-CIT SBR and the BF volume data are the results of general linear model investigating the association between the caudate or putaminal 18F-FP-CIT SBR and the anterior or posterior BF volume, while controlling for age at MRI scan, sex, and disease duration. Results which demonstrated significant correlation are presented in bold.

Figure 1). The PUT_{SBR} was not associated with aBF_{VOL} ($\beta=0.133$, $P=0.085$) but was associated with the pBF_{VOL} ($\beta=0.200$, $P=0.009$). Among the correlation analyses between striatal and BF subregions, the $CAUD_{SBR}$ and pBF_{VOL} demonstrated the most significant association.

Altered brain metabolism in association with striatal dopamine depletion and reduced BF volume

Compared with healthy controls, patients with PD showed increased metabolism in the anterior cingulate cortex and paracentral lobule, whereas decreased metabolism was

observed in the lateral and medial frontal, inferior parietal, lateral and inferior temporal, and lateral and medial occipital cortices, as well as in the precuneus and posterior cingulate cortex. (Figure 2(A)). The $CAUD_{SBR}$ positively correlated with the ^{18}F -FDG SUVR in the lateral frontal, inferior parietal, and medial and lateral occipital cortices, as well as in the precuneus and posterior cingulate cortex (Figure 2(B)). The PUT_{SBR} was positively correlated with nearly identical areas of decreased metabolism in the PD group. The pBF_{VOL} was positively correlated with the ^{18}F -FDG SUVR in the lateral prefrontal, orbito-frontal, inferior parietal, and lateral temporal cortices, as well as in the precuneus, whereas the aBF_{VOL} was not associated with the brain ^{18}F -FDG SUVR. There was a

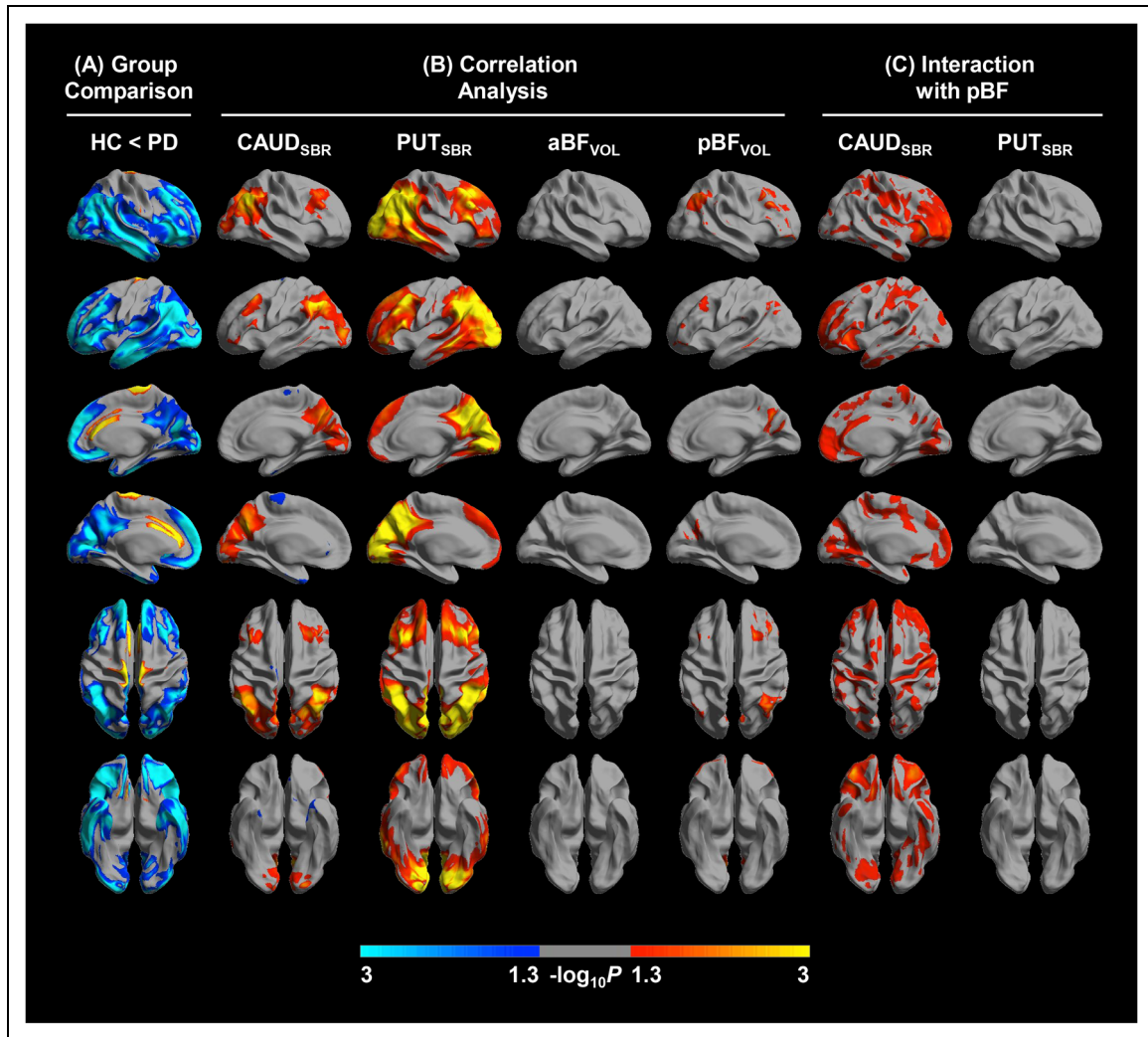


Figure 2. PD-specific, striatal dopamine-related, and BF volume-related brain metabolism (A) group comparison of regional brain ^{18}F -FDG SUVR between healthy controls and patients with PD. (B) Correlation analyses of the striatal ^{18}F -FP-CIT SBR and the BF volume with regional brain ^{18}F -FDG SUVR. (C) Interaction effects of the caudate and putaminal ^{18}F -FP-CIT SBR with the posterior BF volume on regional brain ^{18}F -FDG SUVR. The results are based on a general linear model after controlling for age at ^{18}F -FP-CIT PET, sex, and disease duration. The blue colors in the group comparison represent brain regions with significantly lower ^{18}F -FDG SUVR in the PD group, while the red-to-yellow colors represent brain regions with significantly higher ^{18}F -FDG SUVR in the PD group. The red-to-yellow colors in the correlation analysis indicate brain regions in which the ^{18}F -FDG SUVR positively correlate with the striatal ^{18}F -FP-CIT SBR or the BF volume, while the blue colors indicate brain regions in which the ^{18}F -FDG SUVR negatively correlate with the striatal ^{18}F -FP-CIT SBR or the BF volume. The red colored regions in the interaction analysis of the caudate ^{18}F -FP-CIT SBR are those that demonstrate an interactive effect with the posterior BF volume on regional ^{18}F -FDG SUVR. We presented cortical structures using surface-based analysis.

significant interaction effect between CAUD_{SBR} and pBF_{VOL} on ^{18}F -FDG SUVR in the lateral and medial pre-frontal cortices, as well as the insular, primary sensorimotor, lateral parietal, lateral and anterior temporal, medial and lateral occipital cortices and precuneus (Figure 2(C)). In contrast, there were no significant interaction effects of the pBF_{VOL} and PUT_{SBR} on brain ^{18}F -FDG SUVR.

Association analyses of striatal dopamine depletion and reduced BF volume with cognitive dysfunction

After correction for multiple comparisons, the CAUD_{SBR} was positively correlated with RCFT copy ($\beta=0.32$, $P=0.010$), SVLT immediate ($\beta=0.28$, $P=0.001$) and delayed recall ($\beta=0.25$, $P=0.003$), RCFT delayed recall ($\beta=0.18$, $P=0.014$), COWAT phonemic ($\beta=0.27$,

Table 2. Association of striatal dopamine depletion and basal forebrain atrophy with cognitive dysfunction.

	CAUD _{SBR}		PUT _{SBR}		aBF _{VOL}		pBF _{VOL}		CAUD _{SBR} × pBF _{VOL}	
	β (SE)	P	β (SE)	P	β (SE)	P	β (SE)	P	β (SE)	P
Digit span forward	0.09 (0.08)	0.276	0.14 (0.10)	0.157	6.22 (3.50)	0.077	1.98 (2.13)	0.353	−0.09 (1.31)	0.947
Digit span backward	0.15 (0.08)	0.068	0.15 (0.10)	0.136	10.10 (3.55)	0.005*	6.30 (2.14)	0.004*	0.43 (1.31)	0.745
K-BNT	0.08 (0.07)	0.294	0.01 (0.09)	0.890	2.98 (3.27)	0.364	1.60 (1.98)	0.418	1.46 (1.21)	0.231
RCFT copy	0.32 (0.12)	0.010*	0.38 (0.15)	0.011	9.36 (5.49)	0.090	7.76 (3.28)	0.019*	2.14 (2.00)	0.285
SVLT	0.28 (0.08)	0.001*	0.19 (0.10)	0.057	9.73 (3.65)	0.008*	6.58 (2.19)	0.003*	0.23 (1.32)	0.862
immediate recall										
SVLT delayed recall	0.25 (0.08)	0.003*	0.17 (0.10)	0.106	8.09 (3.77)	0.033	5.99 (2.26)	0.009*	0.43 (1.37)	0.755
SVLT recognition	0.14 (0.09)	0.113	0.14 (0.11)	0.198	4.99 (3.98)	0.212	4.33 (2.39)	0.072	0.23 (1.47)	0.878
RCFT immediate recall	0.16 (0.08)	0.035	0.09 (0.09)	0.363	−0.13 (3.45)	0.971	1.98 (2.07)	0.341	−0.48 (1.27)	0.705
RCFT delayed recall	0.18 (0.07)	0.014*	0.12 (0.09)	0.170	0.09 (3.30)	0.977	2.51 (1.98)	0.206	0.42 (1.20)	0.728
RCFT recognition	−0.01 (0.07)	0.959	−0.01 (0.08)	0.944	−1.92 (2.97)	0.518	−0.31 (1.79)	0.862	−0.99 (1.10)	0.372
COWAT semantic	0.12 (0.06)	0.041	0.08 (0.07)	0.266	4.44 (2.68)	0.099	3.55 (1.60)	0.028	−0.95 (0.98)	0.983
COWAT phonemic	0.27 (0.08)	0.001*	0.24 (0.10)	0.019	5.45 (3.70)	0.142	3.53 (2.23)	0.115	−1.06 (1.34)	0.430
Stroop color reading	0.29 (0.09)	0.001*	0.23 (0.11)	0.035	10.62 (3.87)	0.007*	7.65 (2.31)	0.001*	0.17 (1.40)	0.903

Data are the results of general linear model of the striatal ¹⁸F-FP-CIT SBR or the BF volume with each cognitive item z-score after controlling for age at MR, sex, and disease duration. β is beta coefficient. False discovery rate correction was applied to correct for multiple comparisons. Asterisks indicate significant associations between two variables after false discovery rate correction. Abbreviation = aBF_{VOL}, anterior BF volume; CAUD_{SBR}, caudate ¹⁸F-FP-CIT SBR; COWAT, Controlled Oral Word Association Test; K-BNT, Korean version of the Boston Naming Test; pBF_{VOL}, posterior BF volume; PUT_{SBR}, putaminal ¹⁸F-FP-CIT SBR; RCFT, Rey-Osterrieth Complex Figure Test; SBR, specific binding ratio; SE, standard error; SVLT, Seoul Verbal Learning Test

$P=0.001$), and Stroop color reading z-scores ($\beta=0.29$, $P=0.001$; Table 2). The PUT_{SBR} was not correlated with any cognitive item z-scores. The aBF_{VOL} was positively correlated with digit span backward ($\beta=10.10$, $P=0.005$), SVLT immediate recall ($\beta=9.73$, $P=0.008$), and Stroop color reading z-scores ($\beta=10.62$, $P=0.007$). The pBF_{VOL} was positively correlated with digit span backward ($\beta=6.30$, $P=0.004$), RCFT copy ($\beta=7.76$, $P=0.019$), SVLT immediate ($\beta=6.58$, $P=0.003$) and delayed recall ($\beta=5.99$, $P=0.009$), and Stroop color reading z-scores ($\beta=7.65$, $P=0.001$). However, there was no interaction effect of the CAUD_{SBR} and pBF_{VOL} on cognitive item z-scores.

Association of CAUD_{SBR}- and pBF_{VOL}-related brain metabolism with cognitive dysfunction

After correction for multiple comparisons, both the CAUD_{SBR}-related and pBF_{VOL}-related ¹⁸F-FDG SUVR

showed significant associations with RCFT copy (for CAUD_{SBR}-related ¹⁸F-FDG SUVR, $\beta=1.48$, $P=0.002$; for pBF_{VOL}-related ¹⁸F-FDG SUVR, $\beta=1.50$, $P=0.003$) and Stroop color reading z-scores (for CAUD_{SBR}-related ¹⁸F-FDG SUVR, $\beta=0.96$, $P=0.006$; for pBF_{VOL}-related ¹⁸F-FDG SUVR, $\beta=1.07$, $P=0.003$; Table 3).

Path analyses of cognitive dysfunction

Path analyses revealed that the CAUD_{SBR}-related ¹⁸F-FDG SUVR fully mediated the association between the CAUD_{SBR} and RCFT copy z-score (standardized direct effect, $\beta=0.152$, $P=0.055$; standardized indirect effect, $\beta=0.044$, $P=0.028$) and that the pBF_{VOL}-related ¹⁸F-FDG SUVR fully mediated the association between the pBF_{VOL} and RCFT copy z-score (standardized direct effect, $\beta=0.133$, $P=0.154$; standardized indirect effect, $\beta=0.032$, $P=0.026$; Figure 3(A)). As for Stroop color reading test, the CAUD_{SBR} was associated with Stroop

Table 3. Association of the caudate dopamine-related and the posterior BF volume-related brain metabolism with cognitive dysfunction.

	CAUD _{SBR} -related FDG SUVR		pBF _{VOL} -related FDG SUVR	
	β (SE)	P	β (SE)	P
Digit span forward	0.58 (0.31)	0.067	0.57 (0.32)	0.081
Digit span backward	0.69 (0.32)	0.033	0.70 (0.33)	0.035
K-BNT	0.14 (0.29)	0.632	0.21 (0.30)	0.486
RCFT copy	1.48 (0.48)	0.002*	1.50 (0.50)	0.003*
SVLT immediate recall	0.31 (0.33)	0.358	0.34 (0.34)	0.327
SVLT delayed recall	0.07 (0.34)	0.844	0.09 (0.35)	0.792
SVLT recognition	0.67 (0.35)	0.059	0.67 (0.37)	0.069
RCFT immediate recall	0.46 (0.31)	0.139	0.41 (0.32)	0.195
RCFT delayed recall	0.51 (0.29)	0.083	0.45 (0.30)	0.140
RCFT recognition	0.29 (0.26)	0.271	0.30 (0.27)	0.273
COWAT semantic	0.17 (0.24)	0.487	0.22 (0.25)	0.378
COWAT phonemic	0.53 (0.33)	0.109	0.56 (0.34)	0.101
Stroop color reading	0.96 (0.35)	0.006*	1.07 (0.36)	0.003*

Data are the results of general linear model of the ^{18}F -FDG SUVR in the caudate ^{18}F -FP-CIT SBR-related or the BF volume-related brain regions with each cognitive item z-score after controlling for age at MR, sex, and disease duration. β is beta coefficient. False discovery rate correction was applied to correct for multiple comparisons. Asterisks indicate significant associations between two variables after false discovery rate correction. Abbreviation = CAUD_{SBR}, caudate ^{18}F -FP-CIT SBR; COWAT, Controlled Oral Word Association Test; DR, delayed recall; IR, immediate recall; K-BNT, Korean version of the Boston Naming Test; pBF_{VOL}, posterior BF volume; PUT_{SBR}, putamen ^{18}F -FP-CIT SBR; RCFT, Rey-Osterrieth Complex Figure Test; SBR, specific binding ratio; SE, standard error; SUVR, standardized uptake value ratio; SVLT, Seoul Verbal Learning Test.

color reading z-score both directly and by the mediation of CAUD_{SBR}-related ^{18}F -FDG SUVR (standardized direct effect, $\beta = 0.278$, $P = 0.007$; standardized indirect effect, $\beta = 0.041$, $P = 0.026$; Figure 3(B)). The pBF_{VOL} was also associated with Stroop color reading z-score both directly and by the mediation of pBF_{VOL}-related ^{18}F -FDG SUVR (standardized direct effect, $\beta = 0.248$, $P = 0.005$; standardized indirect effect, $\beta = 0.032$, $P = 0.041$).

Discussion

In this study, we investigated the relationship between striatal dopamine depletion, cholinergic BF volume atrophy, altered brain metabolism, and cognitive dysfunction in patients with PD. The major findings were as follows. First, caudate dopamine depletion was associated with posterior BF atrophy. Second, both caudate and putamen dopamine depletion were associated with altered brain metabolism in regions where PD patients showed decreased metabolism compared with healthy controls, whereas atrophy in the posterior BF was associated with reduced brain metabolism in the lateral

prefrontal, orbitofrontal, inferior parietal, and lateral temporal cortices, as well as in the precuneus, with a significant interaction between caudate DAT availability and the pBF_{VOL}. Third, caudate dopamine depletion was associated with visuospatial, memory, and executive dysfunction, while BF atrophy, especially in the posterior region, was associated with attention, visuospatial, memory, and executive dysfunction. Fourth, visuospatial dysfunction was associated with caudate dopamine depletion and posterior BF atrophy through the mediation of altered brain metabolism, whereas executive dysfunction was associated with caudate dopamine depletion and posterior BF atrophy both directly and by the mediation of altered brain metabolism. Taken together, in PD, dopamine depletion in the caudate and BF atrophy in the posterior part were closely related and affected item-specific cognitive dysfunction, either directly or through the mediation of altered brain metabolism.

Based on the volumetric analysis of BF subregions using the cytoarchitectonic atlas of BF cholinergic nuclei, we discovered a significant correlation between striatal dopamine uptake and the pBF_{VOL}. Our results may reflect the simultaneous invasion of PD-related pathology into the magnocellular cholinergic neurons of the BF and dopaminergic neurons of the midbrain,²⁴ and they support prior research showing that dopaminergic and cholinergic deficits progress in tandem in PD.^{25,26} Furthermore, significant relationships found in compromised midbrain dopaminergic and BF cholinergic neurons may even suggest direct monoaminergic-cholinergic interactions between them. It has already been discovered that brainstem cholinergic neurons regulate the firing rate of midbrain dopaminergic neurons²⁷ and that BF cholinergic neurons are targeted by dopaminergic neurons in the midbrain.²⁸ Our results may be the *in vivo* evidence of a close interplay between midbrain dopaminergic and BF cholinergic neurons. Additional studies are required to elucidate the mechanisms by which both neurotransmitter systems deteriorate in patients with PD.

Previous studies exploring the relationship between brain metabolism and nigrostriatal degeneration have reported heterogeneous results. In one study, striatal dopamine depletion was associated with more pronounced PD-related patterns (PDRP),²⁹ while others reported altered metabolism in more circumscribed regions, such as the bilateral medial frontal cortices,³⁰ right cerebellum, and fusiform gyrus.³¹ The current study demonstrated that regions of hypometabolism associated with striatal dopamine depletion resembled PD-related patterns topography, similar to previous studies.^{16,29} Our results suggest that dopaminergic alterations may be primarily responsible for most of the cortical metabolic changes characteristic of PD.

As for altered metabolism in dopamine-unrelated regions, such as the anterior and medial temporal, insular, and cingulate cortices, we examined whether BF cholinergic deficits could be responsible for hypometabolism in these regions. Previous studies exploring the role of BF atrophy in altered

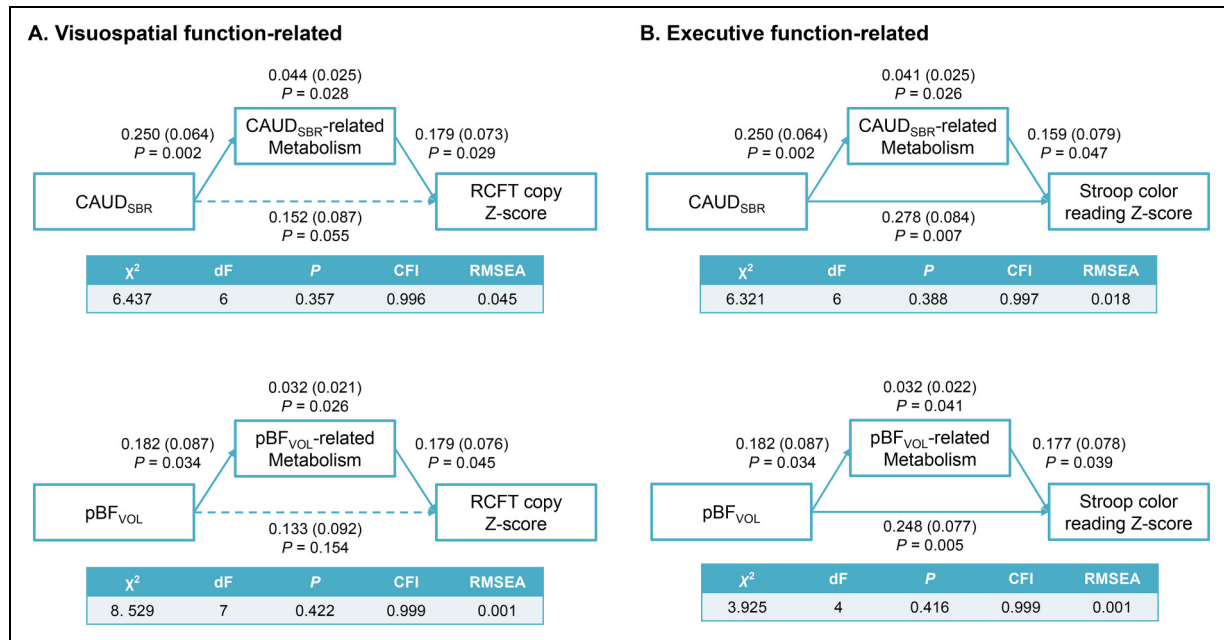


Figure 3. Path analyses of the association of the posterior BF volume or caudate I8F-FP-CIT SBR with brain I8F-FDG SUVR and cognitive dysfunction in PD. Schematic diagram of the path analysis for (A) the RCFT copy z-score and (B) the Stroop color Reading z-score. Age at I8F-FP-CIT PET, sex, and disease duration were used as common covariates. The pBFVOL was used as an additional covariate when CAUDSBR was a predictor, while the CAUDSBR was used as an additional covariate when pBFVOL was a predictor. Values above or below lines are standardized regression coefficient, standard error, and significance probability of direct effects. Values above boxes are standardized regression coefficient, standard error, and significance probability of indirect effects. Solid lines indicate significant path, while dashed lines indicate insignificant path. Abbreviations = CFI, comparative fit index; dF, degree of freedom; RMSEA, root mean square error of approximation.

brain metabolism exhibited heterogeneous results. One study that included MCI patients reported the association of widespread hypometabolism in the bilateral limbic, paralimbic, and heteromodal association cortices with lower total BF volume.³² When the nucleus basalis of Meynert volume was used instead of total BF volume in another study on PD patients, however, hypometabolism was demonstrated only in the parietal and occipital cortices.¹⁷ We further divided the BF into anterior and posterior parts, unlike the aforementioned studies, and examined their relationship with altered brain metabolism. Our study revealed that hypometabolism in the lateral prefrontal, orbitofrontal, inferior parietal, and lateral temporal cortices and the precuneus was specifically associated with atrophy in the posterior BF, and the aBF_{VOL} demonstrated no correlation with brain metabolism. Our results suggest that hypometabolism in these regions may be attributed to the degeneration of the posterior BF followed by cortical cholinergic denervation. Furthermore, it is of note that the lateral prefrontal and parietal regions comprise the central executive network.³³ As the central executive network plays a critical role in sustained attention and executive function,³⁴ our findings suggest a potential link between BF cholinergic degeneration and central executive network dysfunction, thereby contributing to attentional and executive deficits in PD.

We additionally investigated whether there was an interaction effect between striatal dopamine uptake and the posterior BF volume on brain metabolism, as we have previously discovered a significant relationship between the two. Interestingly, our analyses showed that caudate, but not putamen, dopamine depletion had an interactive effect with posterior BF atrophy on reduced metabolism in widespread brain regions, especially in the prefrontal region. This result is significant because it suggests an interplay between the caudate and BF in disease progression and clinical worsening. A previous study investigating clinical heterogeneity in early PD patients based on the level of caudate dysfunction revealed that more reduced caudate dopamine uptake was associated with lower MoCA scores at the 4-year follow-up while no difference was found between each group at baseline.⁸ It proposed that caudate dopaminergic deficits that were not severe enough at baseline later predisposed to clinical symptoms in combination with degeneration in other neurotransmitter systems. In line with this hypothesis, our results may demonstrate how the interaction between dopamine and acetylcholine contributes to heterogeneous progression patterns observed in PD. Interestingly, no interaction effects of these neurotransmitters on cognition were found in this cross-sectional study. It is possible that while they may interact in

influencing brain metabolism, such an interaction may not extend directly to cognitive impairment. Further studies are needed to examine whether mitigating the deterioration of either neurotransmitter system improves overall brain metabolism and ultimately affects clinical prognosis.

The association between dopamine depletion in the caudate and cognitive decline has been discussed in multiple studies, all reporting heterogeneous results.^{4,8,35,36} A multicenter cohort study revealed that nigrostriatal dopaminergic activity was related to executive function but not to memory or visuospatial function.³⁶ These results align with a previous theory that frontostriatal dopaminergic deficits contribute to executive dysfunction, while visuospatial function and memory are more likely to be affected by cholinergic deficits. However, more recent research has demonstrated that decreased DAT availability in the caudate is associated with memory and visuospatial impairment in addition to executive dysfunction.⁴ The effects of BF atrophy on cognitive dysfunction also varied between studies depending on the specific BF subregion analyzed. Reduced volume of the nucleus basalis of Meynert was associated with worse executive and visuospatial functions,¹⁷ while loss of structural integrity in Ch 1-2 was correlated with memory test scores, and changes in Ch 3-4 were associated with global cognition and executive function scores.¹⁰ Our findings were consistent with those of previous studies in which smaller BF volumes, either Ch4 or total, correlated with worse memory, attention/executive, and visuospatial function.^{9,32} Together with our results, we can infer from these findings that cognitive impairments in PD should not be considered as a consequence of single neurotransmitter dysfunction but should be explained as the sum of multiple neurotransmitter deficits and their related brain dysfunction. Intriguingly, we found no interaction effects between caudate dopamine deficits and posterior BF atrophy on cognition. This contrasts with the previous finding that showed significant interactive effects of caudate dopaminergic and cortical cholinergic deficits.³⁷ A possible explanation for this discrepancy could be that carbon 11-labeled methyl-4-piperidinyl propionate acetylcholinesterase PET was used in the previous study, which is more sensitive than BF volume in detecting cholinergic deficits. This methodological distinction may account for the observed differences in the interaction analysis. Furthermore, the disease duration in our cohort of patients was shorter (mean \pm SD disease duration 3.63 ± 4.07 years) than that in the previous study (mean \pm SD disease duration 6.0 ± 4.3 years). It has been observed that cortical cholinergic denervation occurs mainly in patients with significant caudate nucleus dopaminergic denervation, and that dopaminergic denervation induces compensatory overactivity of cortical cholinergic afferents.^{37,38} Because patients with advanced PD or PD dementia were likely underrepresented in this study, drawing conclusive results regarding interactive effects of dopamine and acetylcholine on

cognition may have been limited. Future studies should be conducted with a larger sample size and wider spectrum of cognitive dysfunction.

Our path analyses revealed that brain hypometabolism mediates the relationship between caudate dopamine depletion or posterior BF cholinergic deficits and specific cognitive dysfunction. While it has been established that brain hypometabolism mediates the effects of AD-related pathology on cognition and is regarded as a marker of neurodegeneration,^{39,40} the temporal framework of the progression of Lewy body pathologies into overt cognitive decline is still not well defined. Our group has previously highlighted the possible role of brain metabolism in mediating dopamine depletion and specific cognitive domains in PD¹⁶ and dementia with Lewy bodies.⁴¹ In the current study, we demonstrated that visuospatial function in PD was not directly affected by striatal dopaminergic or BF cholinergic deficits but was fully mediated by brain hypometabolism. Executive dysfunction was partly directly associated with striatal dopaminergic or BF cholinergic deficits but was also mediated by brain hypometabolism. These results suggest that changes in brain metabolism in relation to caudate dopamine depletion and posterior BF atrophy should be incorporated when evaluating PD-specific cognitive impairments. Moreover, our path analyses may explain why dopamine and acetylcholine did not demonstrate synergistic effects on cognition in the current study. It is possible that altered brain metabolism is the direct determinant of cognitive dysfunction, rather than the neurotransmitter deficits themselves, which primarily influence cognition through metabolic changes. Their deterioration may synergistically result in significant metabolic decline, which in turn ultimately manifests as cognitive impairment. Analyses with larger samples and external validation will be required to enhance the reliability and generalizability of these findings.

The present study had several limitations. First, it included only cross-sectional data and lacked longitudinal observations to confirm the sequential relationship between caudate dopamine depletion or posterior BF atrophy, altered brain metabolism, and cognitive impairments. Detailed longitudinal neuropsychological tests and imaging studies may validate the temporal framework proposed in this study. Second, co-pathologies, such as Alzheimer's disease pathology, were not considered. Third, while dopamine depletion was assessed as a functional deficit using PET, cholinergic deficits were evaluated only structurally based on BF atrophy. Future studies using PET or other imaging modalities to assess cholinergic deficits are required, as they may further reveal underlying interaction effect between caudate dopamine and BF cholinergic depletion on cognition. Fourth, the study group consisted of patients with relatively shorter disease durations, and they were also not genetically screened for monogenic mutations, although certain genetic mutations have been reported to exert distinct effects on brain metabolism.⁴²

Future studies incorporating wider spectrum of cognitive dysfunction and genetic influences will be necessary. Fifth, this study was conducted only in a single center and exclusively in the Korean population; therefore, there is an inherent limitation regarding the generalizability of the findings. Multi-center study or cross-ethnic validation may strengthen the external validity of the finding. Sixth, different MRI scanners and protocols were used for healthy controls while comparing metabolic changes with the PD group.

In summary, our study demonstrated that dopamine depletion in the caudate and atrophy in the posterior BF affect brain metabolism and cognition, with or without interaction effects, and that alterations in cortical metabolic activities mediate the impact of dopaminergic and cholinergic denervation on cognitive dysfunction in a domain-specific manner. This highlights the importance of considering the dysfunction of multiple neurotransmitter systems, as well as decreased brain metabolism, to understand cognitive dysfunction in patients with PD.

Acknowledgements

None

Author contributions

J.H.L., H.S.Y. and C.H.L. contributed to the conception and design of the study; J.H.L., H.S.Y., C.H.L., S.J.A., M.P., J.H.L., Y.H.R contributed to the data acquisition; J.H.L., H.S.Y., C.H.L contributed to the data analysis; J.H.L., H.S.Y., C.H.L contributed to drafting the manuscript.

Funding

This research was supported by a grant of the Korea Health Technology R&D Project through the Korea Health Industry Development Institute (KHIDI), funded by the Ministry of Health & Welfare, South Korea (grant number: RS-2023-00266536).

Korea Health Industry Development Institute, (grant number RS-2023- 00266536).

Declaration of conflicting interests

The authors declared no potential conflicts of interest with respect to the research, authorship, and/or publication of this article.


Data availability

To replicate the procedures and results, any qualified investigator can request anonymized data after obtaining ethics clearance and approval from all authors.

ORCID iDs

Jung Hyun Lee  <https://orcid.org/0000-0001-5082-1075>

Jae Hoon Lee  <https://orcid.org/0000-0002-9898-9886>

Chul Hyoung Lyoo  <https://orcid.org/0000-0003-2231-672X>

Disclosure

The authors report no disclosure relevant to the manuscript.

Supplemental material

Supplemental material for this article is available online.

References

1. Dickson DW. Neuropathology of Parkinson disease. *Parkinsonism Relat Disord* 2018; 46: S30–s33.
2. Schapira AHV, Chaudhuri KR and Jenner P. Non-motor features of Parkinson disease. *Nat Rev Neurosci* 2017; 18: 435–450.
3. Chaudhuri KR, Healy DG and Schapira AH. Non-motor symptoms of Parkinson's disease: diagnosis and management. *Lancet Neurol* 2006; 5: 235–245.
4. Chung SJ, Yoo HS, Oh JS, et al. Effect of striatal dopamine depletion on cognition in de novo Parkinson's disease. *Parkinsonism Relat Disord* 2018; 51: 43–48.
5. Hobson P, Meara J and Ishihara-Paul L. The estimated life expectancy in a community cohort of Parkinson's disease patients with and without dementia, compared with the UK population. *J Neurol Neurosurg Psychiatry* 2010; 81: 1093–1098.
6. de Lau LM, Verbaan D, Marinus J, et al. Survival in Parkinson's disease. Relation with motor and non-motor features. *Parkinsonism Relat Disord* 2014; 20: 613–616.
7. Aarsland D, Creese B, Politis M, et al. Cognitive decline in Parkinson disease. *Nature Reviews Neurology* 2017; 13: 217–231.
8. Pasquini J, Durcan R, Wiblin L, et al. Clinical implications of early caudate dysfunction in Parkinson's disease. *J Neurol Neurosurg Psychiatry* 2019; 90: 1098–1104.
9. Barrett MJ, Sperling SA, Blair JC, et al. Lower volume, more impairment: reduced cholinergic basal forebrain grey matter density is associated with impaired cognition in Parkinson disease. *J Neurol Neurosurg Psychiatry* 2019; 90: 1251–1256.
10. Gargouri F, Gallea C, Mongin M, et al. Multimodal magnetic resonance imaging investigation of basal forebrain damage and cognitive deficits in Parkinson's disease. *Mov Disord* 2019; 34: 516–525.
11. Bohnen NI and Albin RL. The cholinergic system and Parkinson disease. *Behav Brain Res* 2011; 221: 564–573.
12. Liu AK, Chang RC, Pearce RK, et al. Nucleus basalis of meynert revisited: anatomy, history and differential involvement in Alzheimer's and Parkinson's disease. *Acta Neuropathol* 2015; 129: 527–540.
13. Crowley SJ, Kanel P, Roytman S, et al. Basal forebrain integrity, cholinergic innervation and cognition in idiopathic Parkinson's disease. *Brain* 2023; 147: 1799–1808.
14. Höglinger GU, Adler CH, Berg D, et al. A biological classification of Parkinson's disease: the SynNeurGe research diagnostic criteria. *Lancet Neurol* 2024; 23: 191–204.
15. Huang C, Mattis P, Perrine K, et al. Metabolic abnormalities associated with mild cognitive impairment in Parkinson disease. *Neurology* 2008; 70: 1470–1477.
16. Yoo HS, Kim HK, Na HK, et al. Association of striatal dopamine depletion and brain metabolism changes with motor and cognitive deficits in patients with Parkinson disease. *Neurology* 2024; 103: e210105.

17. Gang M, Baba T, Hosokai Y, et al. Clinical and cerebral metabolic changes in Parkinson's disease with basal forebrain atrophy. *Mov Disord* 2020; 35: 825–832.
18. Postuma RB, Berg D, Stern M, et al. MDS Clinical diagnostic criteria for Parkinson's disease. *Mov Disord* 2015; 30: 1591–1601.
19. Fazekas F, Chawluk JB, Alavi A, et al. MR Signal abnormalities at 1.5T in Alzheimer's dementia and normal aging. *AJR Am J Roentgenol* 1987; 149: 351–356.
20. Ahn HJ, Chin J, Park A, et al. Seoul Neuropsychological screening battery-dementia version (SNSB-D): a useful tool for assessing and monitoring cognitive impairments in dementia patients. *J Korean Med Sci* 2010; 25: 1071–1076.
21. Kilimann I, Grothe M, Heinsen H, et al. Subregional basal forebrain atrophy in Alzheimer's disease: a multicenter study. *J Alzheimers Dis* 2014; 40: 687–700.
22. Fritz HJ, Ray N, Dyrba M, et al. The corticotopic organization of the human basal forebrain as revealed by regionally selective functional connectivity profiles. *Hum Brain Mapp* 2019; 40: 868–878.
23. Desikan RS, Ségonne F, Fischl B, et al. An automated labeling system for subdividing the human cerebral cortex on MRI scans into gyral based regions of interest. *Neuroimage* 2006; 31: 968–980.
24. Braak H, Del Tredici K, Rüb U, et al. Staging of brain pathology related to sporadic Parkinson's disease. *Neurobiol Aging* 2003; 24: 197–211.
25. Bohnen NI, Yarnall AJ, Weil RS, et al. Cholinergic system changes in Parkinson's disease: emerging therapeutic approaches. *Lancet Neurol* 2022; 21: 381–392.
26. Müller ML and Bohnen NI. Cholinergic dysfunction in Parkinson's disease. *Curr Neurol Neurosci Rep* 2013; 13: 377.
27. Mena-Segovia J, Winn P and Bolam JP. Cholinergic modulation of midbrain dopaminergic systems. *Brain Res Rev* 2008; 58: 265–271.
28. Zaborszky L and Cullinan WE. Direct catecholaminergic-cholinergic interactions in the basal forebrain. I. Dopamine-beta-hydroxylase- and tyrosine hydroxylase input to cholinergic neurons. *J Comp Neurol* 1996; 374: 535–554.
29. Holtbernd F, Ma Y, Peng S, et al. Dopaminergic correlates of metabolic network activity in Parkinson's disease. *Hum Brain Mapp* 2015; 36: 3575–3585.
30. Apostolova I, Lange C, Frings L, et al. Nigrostriatal degeneration in the cognitive part of the Striatum in Parkinson disease is associated with frontomedial hypometabolism. *Clin Nucl Med* 2020; 45: 95–99.
31. Kim R, Kim H, Kim YK, et al. Brain metabolic correlates of dopaminergic denervation in prodromal and early Parkinson's disease. *Mov Disord* 2022; 37: 2099–2109.
32. Grothe MJ, Heinsen H and Amaro E Jr, Initiative ftAsDN. Cognitive correlates of basal forebrain atrophy and associated cortical hypometabolism in mild cognitive impairment. *Cereb Cortex* 2015; 26: 2411–2426.
33. Cao W, Cao X, Hou C, et al. Effects of Cognitive Training on Resting-State Functional Connectivity of Default Mode, Salience, and Central Executive Networks. *Front Aging Neurosci* 2016; 8: 70.
34. Seeley WW, Menon V, Schatzberg AF, et al. Dissociable intrinsic connectivity networks for salience processing and executive control. *J Neurosci* 2007; 27: 2349–2356.
35. Arnaldi D, Campus C, Ferrara M, et al. What predicts cognitive decline in de novo Parkinson's disease? *Neurobiol Aging* 2012; 33: 1127.e1111–1120.
36. Siepel FJ, Brønneck KS, Booij J, et al. Cognitive executive impairment and dopaminergic deficits in de novo Parkinson's disease. *Mov Disord* 2014; 29: 1802–1808.
37. Bohnen NI, Albin RL, Müller ML, et al. Frequency of cholinergic and caudate nucleus dopaminergic deficits across the predemented cognitive spectrum of Parkinson disease and evidence of interaction effects. *JAMA Neurol* 2015; 72: 194–200.
38. Kim K, Bohnen NI, Müller M, et al. Compensatory dopaminergic-cholinergic interactions in conflict processing: evidence from patients with Parkinson's disease. *Neuroimage* 2019; 190: 94–106.
39. Mattsson N, Insel PS, Aisen PS, et al. Brain structure and function as mediators of the effects of amyloid on memory. *Neurology* 2015; 84: 1136–1144.
40. Saint-Aubert L, Almkvist O, Chiotis K, et al. Regional tau deposition measured by [(18)F]THK5317 positron emission tomography is associated to cognition via glucose metabolism in Alzheimer's disease. *Alzheimers Res Ther* 2016; 8: 38.
41. Yoo HS, Jeong SH, Oh KT, et al. Interrelation of striatal dopamine, brain metabolism and cognition in dementia with Lewy bodies. *Brain* 2022; 145: 4448–4458.
42. Greuel A, Trezzi JP, Glaab E, et al. GBA Variants in Parkinson's disease: clinical, metabolomic, and multimodal neuroimaging phenotypes. *Mov Disord* 2020; 35: 2201–2210.